



Improved Performance Analysis of Single-phase Line Start Synchronous Reluctance Motor Derived from Induction Motor

M. Chaudhari*, A. Chowdhury

Department of Electrical Engineering, Sardar Vallabhbhai National Institute of Technology, Surat, Gujarat, India

PAPER INFO

Paper history:

Received 12 August 2021

Received in revised form 03 May 2022

Accepted 22 May 2022

Keywords:

Barrier

Parametric Analysis

Motor Efficiency

Finite Element Analysis

ABSTRACT

Energy efficiency is an essential aspect of motor technologies. The replacement of conventional Single Phase Induction Motor (SPIM) by Permanent Magnet Synchronous Motor (PMSM), Synchronous Reluctance Motor (SynRM), or Switched Reluctance Motor (SRM) for energy-efficient operation leads to high capital expenses. This paper presents a cost-effective design method to improve the efficiency of the existing SPIM. It implements a novel idea by transforming it to Line Start Synchronous Reluctance Motor (LS-SynRM). A rotor of 0.5 HP, SPIM is successfully redesigned using finite element analysis (FEA). A comprehensive parametric sensitivity analysis in terms of barrier position and width focused on the work. Moreover, introducing a permanent magnet in the rotor barrier has also been investigated. Parametric analysis determines the optimum size of the permanent magnet. However, the best-fit significant rotor parameters have been estimated. Results revealed substantial improvement in the performance of derived LS-SynRM and Permanent Magnet Assisted LS-SynRM (PMaLS-SynRM).

doi: 10.5829/ije.2022.35.08b.20

NOMENCLATURE

| | | | |
|-------------|---|--------------|---------------------------|
| ψ | Flux linkages | P_{cu} | Copper losses |
| β | Winding displacement between auxiliary and main winding | P_{core} | Core losses |
| α | Turns ratio | P_{core-s} | Stator core loss |
| m | Number of phases | I_L | Line current |
| p | Number of poles | I_m | Main winding current |
| L_d | Direct axis inductance | I_a | Auxiliary winding current |
| L_q | Quadrature axis inductance | | |
| T_e | Electromagnetic torque | | |
| T_{cage} | Cage torque | | |
| T_{rel} | Reluctance torque | | |
| P_{mech} | Mechanical output power | | |
| P_{elect} | Electrical input power | | |

| Greek Symbols | | | |
|----------------------|------------|--|--|
| η | Efficiency | | |

| Subscripts | | | |
|-------------------|-----------------|--|--|
| d | Direct axis | | |
| q | Quadrature axis | | |

1. INTRODUCTION

Single-phase induction motors (SPIM) have widespread applications. However, there is growing interest in

energy-efficient motors like PMSMs, SRMs, and SynRMs, although it incurs a cost to the user [1]. Many research studies reported in the literature attempted to improve the performance of induction motors in terms of

*Corresponding Author Institutional Email:
mandar.chaudhari@ges-coengg.org (M. Chaudhari)

the introduction of slits in the teeth, magnetic wedges, use of nanomaterial, and high-grade steel to reduce the losses [2-5]. Although these methods improve efficiency, it also leads to increased manufacturing difficulties added with material cost. However, PMSMs, SRMs, and SynRMs, although energy-efficient, line-starting capability is still under investigation.

The option of single-phase operation of three-phase induction motors has also been investigated [6, 7] to retrieve the benefits of three-phase IM. The research reported by Chaudhari and Fernandes [8] also considers the same principle for PMSM with a reduction in thirty percent output. The work presented by Gwoźdiewicz and Zawilak [9] uses skewed stator slots to enhance the performance; however, it reduces noise with trivial improvements in the performance. However, the availability of high-density permanent magnets for PMSM motors at low cost is a significant concern.

The motors like SRM and SynRM [10, 11] have superior features compared with PMSM, like reduced cost and better performance. However, their line starting ability is still a research interest.

The absence of rotor bars and permanent magnets makes the SRM rugged in construction and efficient. However, it demands the converter and rotor position sensors for operation [12, 13], increasing complexity and cost. Line starting with a simple diode rectifier [14] significantly compromises the efficiency.

In synchronous motors like SynRM, the current induced in the rotor at synchronization is absent. It leads to negligible rotor copper loss resulting inefficient operation. As SynRMs are realized by replacing SPIM rotors [15-23], efficient performance is obtained at a reduced cost than the PMSM. The energy density and performance are better for these motors than induction motors [15]. The new rotor design [16] further improves the polyphase operation performance. The analytical investigations into line start single phase SynRM using rotating field theory [22], and symmetrical components analysis in transient and steady-state is presented [17].

Self-starting single-phase SynRM with barriers and with cage bars designed and analyzed by Gu and Zhou [19]. The operation of a single-phase cage rotor reluctance motor with a variable capacitor is presented by Obe and Oje [20], considering speed error signal as feedback. However, an additional control circuit in the feedback loop and the variable capacitor increases the system cost. Recently, Ganesan and Chokkalingam [21] developed line start single-phase synchronous reluctance motor records 6% increase in efficiency than SPIM. Aghazadeha et al. [23] compared the permanent magnet assisted SynRM (PMaSynRM) with SynRM without PM. It has superior performance in terms of torque profile. However, all of these analyses use the newly manufactured rotor to improve performance. Moreover, adding active material in motor structure or replacing the

motor with energy-efficient motor results in increased cost.

This literature review reveals comparatively less attention to the online operation of single-phase SynRM. However, the attention given to improve the efficiency of SPIM without manufacturing a new rotor is scant. A novel concept reported in this paper considers these research gaps. It derives LS-SynRM from the existing SPIM rotor itself. The investigation of optimum barrier dimensions is determined through parametric analysis. The parameters such as placement of the barrier, its width, and rib dimensions were examined. The conversion of SPIM to LS-SynRM, without the requirement for additional material and little modification cost, is an economically viable option. In addition, considering the advantages of high-density permanent magnets, the effect of adding pieces of permanent magnets in the rotor is investigated. The performance, in this case, is compared for varying lengths of the magnets. The performed analysis also determines the best-fit magnet configuration with improved efficiency for the PMaLS-SynRM.

In section 2, a brief introduction of line start SynRM is given in this paper. In section 3 proposed design procedure of line start, SynRM is described. Section 4 deals with single-phase 0.5HP motor simulation in Ansys Maxwell for rated load condition and FEM-based sensitivity analysis of rotor structures for different parameters with simulation results such as synchronizing capability, torque, losses, and efficiency. The conclusion is given in section 5.

2. SINGLE PHASE LINE START SYNCHRONOUS RELUCTANCE MOTOR

The stator structure is kept the same for the proposed conversion of SPIM to LS-SynRM. The main and auxiliary windings displaced through 90° in space. Two capacitors, starting and running, are connected in the circuit. The starting capacitor is connected with auxiliary winding through a centrifugal switch to start the machine directly online. A low-value run capacitor is left in the auxiliary winding for better performance.

The starting torque (T_{cage}) developed by the rotor cage makes the motor line start while the reluctance torque (T_{rel}) maintains synchronism [18].

The flux linkage equations in the d-q reference frame for FEM analysis [24] and flux linkages along the dq axis are stated in Equation (1).

$$\begin{bmatrix} \psi_d \\ \psi_q \end{bmatrix} = \begin{bmatrix} \cos\theta & \sin\theta \\ -\sin\theta & \cos\theta \end{bmatrix} \begin{bmatrix} 1 & 0 \\ 0 & 1/\alpha \end{bmatrix} \begin{bmatrix} 1 & \cos\beta \\ 0 & \sin\beta \end{bmatrix} \begin{bmatrix} \psi_{as} \\ \psi_{bs} \end{bmatrix} \quad (1)$$

where α indicates auxiliary to main winding turns ratio and β represents winding displacement between auxiliary

and main winding and ψ_{as} , ψ_{bs} is flux linkages of stator 'a' phase and stator 'b' phase respectively.

The current in d-q frame is also given in Equations (2) and (3):

$$i_d = i_a \cos \theta + i_b [\cos \theta \cdot \cos \beta + \alpha \cdot \sin \theta \cdot \sin \beta] \quad (2)$$

$$i_q = i_a \sin \theta - i_b [-\sin \theta \cdot \cos \beta + \alpha \cdot \cos \theta \cdot \sin \beta] \quad (3)$$

Knowing the flux linkages and currents, the inductances along the direct and quadrature axis are given by-

$$L_d = \frac{\psi_d}{i_d} \quad (4)$$

$$L_q = \frac{\psi_q}{i_q} \quad (5)$$

Then equation for electromagnetic torque can be expressed as follows:

$$T_e = T_{cage} + T_{rel} \quad (6)$$

$$T_e = \frac{m}{2} \frac{p}{2} \frac{L_m}{L_r} L_m i_d + \frac{m}{2} \frac{p}{2} (L_d - L_q) i_d i_q \quad (7)$$

where,

T_e - Electromagnetic torque

L_m - Magnetizing inductance

p - Number of Poles

m - Number of phases

L_d, L_q - Direct axis and quadrature axis inductance

i_d, i_q - Direct axis and quadrature axis current

The steady state efficiency is calculated by the ratio of output mechanical power (P_{mech}) and input electrical power (P_{elect}).

$$\eta = \frac{P_{mech}}{P_{elect}} = \frac{P_{mech}}{P_{mech} + P_{cu} + P_{core} + \text{other losses}} \quad (8)$$

where P_{mech} is calculated as Equation (9):

$$P_{mech} = (\text{Torque}) \times (\text{angular speed}) \quad (9)$$

While friction, windage losses are assumed to be 1.2% and stray losses are considered 1% of output power. The addition of copper losses (P_{cu}), core losses (P_{core}), and other losses computes total loss.

Total copper loss is the summation of auxiliary and main winding copper loss and rotor copper loss. Total core losses include stator and rotor core loss. Consequently, Equation (10) determines the input electrical power.

$$P_{elect} = (P_{mech}) + (P_{cu}) + (P_{core}) + (\text{other loss}) \quad (10)$$

Other loss includes friction, windage losses and stray losses.

3. PROPOSED DESIGN PROCEDURE

3. 1. Design Method

A new LS-SynRM design aims to replace an existing single-phase IM subjected to two aspects. Firstly, it has to have line-starting and successful synchronization. Second, the motor should have higher or equal torque and higher efficiency at a steady-state than the existing single-phase IM. The FE analysis considers the FB design and its effect on performance and motor parameters. The parametric design variables considered for analysis are barrier position, barrier width, and PM size. The evaluated efficiency and torque are then compared with base SPIM. The design steps undertaken prescribed in Figure 1. The

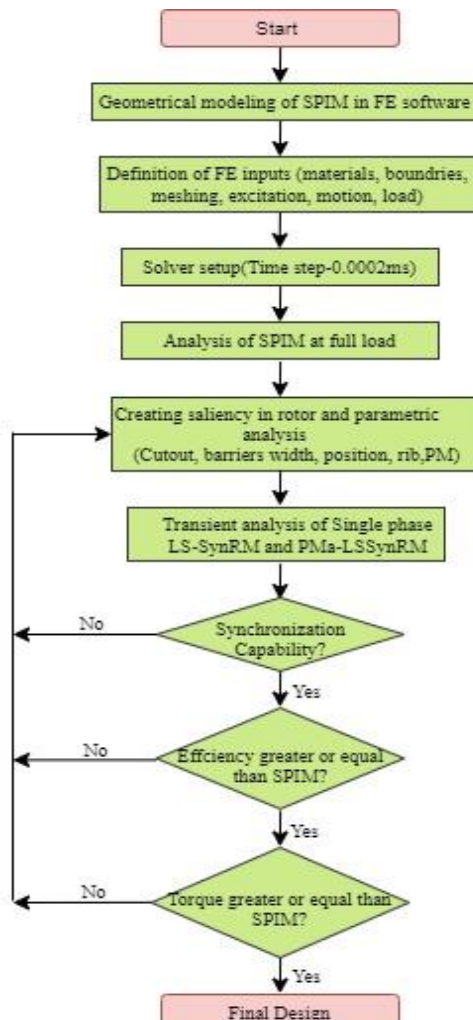


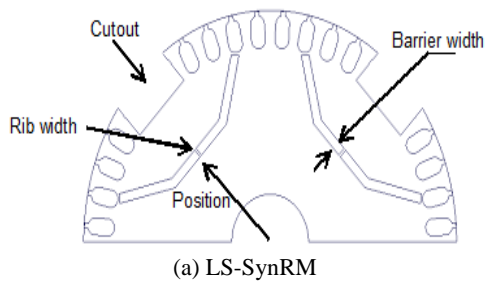
Figure 1. Design and analysis procedure

base SPIM first analyzed at rated load condition. The modified rotor with barriers has been examined with various barrier and PM dimensions as described in Figures 2(a) and 2(b). Each of the examined model was checked for synchronization ability, efficiency and torque. The model that satisfies above three criterions were compared. The model satisfying set criterions and higher efficiency than SPIM designated as best fit model.

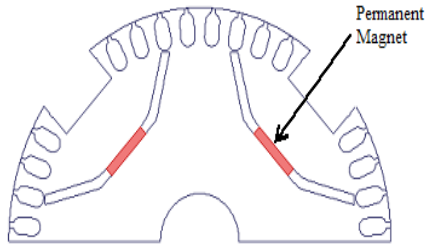
3.2. Simulation Model The motor models with structural dimensions are realized using ANSYS Maxwell™ FE analysis software. The material used for the rotor cage is aluminum, while the stator winding conductors are of copper. The half-section automatic adaptive mesh models, as shown in Figure 3, are generated considering the memory requirements. The mesh elements generated were 6742 for SPIM and that for LS-SynRM was 6824. The external excitation circuit is coupled with a voltage of single-phase 230V.

4. RESULTS AND DISCUSSION

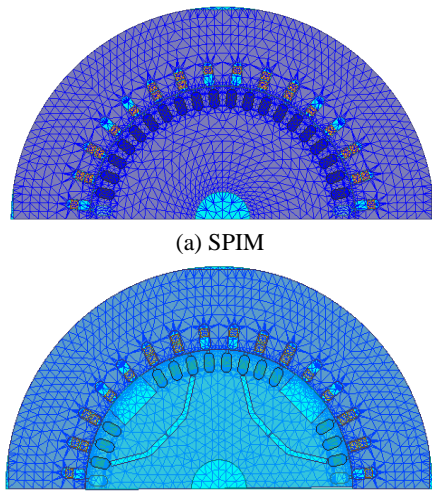
The relative performance presented in this section is for SPIM, LS-SynRM, and PMaLS-SynRM.



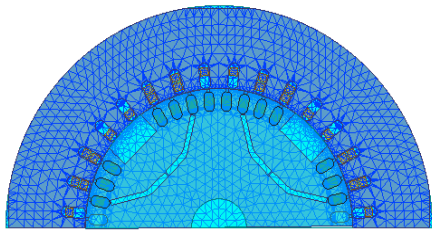
(a) LS-SynRM



(b) PMaLS-SynRM

Figure 2. Rotor structures

(a) SPIM



(b) LS-SynRM

Figure 3. Mesh models (a) SPIM and (b) line start SynRM

4. 1. Base Motor Analysis

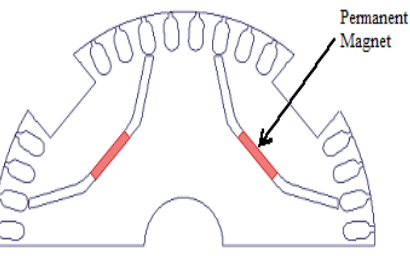
A single-phase induction motor (SPIM) is used as a base motor for comparative analysis in this study. Rated as 230V, 50 Hz, 0.5HP, 1440 rpm, capacitor start-capacitor run induction motor modeled in software as shown in Figure 4. The starting and running capacitor values were 70 μ F and 15 μ F, respectively. The constructive parameters have been specified in Table 1.

The transient performance analysis of torque, speed, mechanical power output and losses have been analyzed under full load conditions. Figure 5 shows the significant performance characteristics. The evaluated core loss, stator copper losses, and rotor copper losses are 31.72W, 33.1W, and 22.9W, respectively, with the mechanical power developed as 387.83W. The full load torque developed was 2.55N-m at a speed of 1447rpm, where the efficiency noted was 80.12%. The other losses calculated are 2.2 percent of rated output power.

4. 2. LS-SynRM Motor Analysis

4. 2. 1. Parametric Sensitivity Analysis for Barrier Positions and Width

The total 24 models, including six width sizes for each of the four barrier positions, are created and analyzed. The width was

**TABLE 1.** Geometrical dimensions of SPIM

| Parameter | Dimension | Parameter | Dimension |
|-----------------------|-----------|------------------------|-----------|
| Stator outer diameter | 152mm | Rotor outside diameter | 91.4mm |
| Bore Diameter | 92mm | Number of stator slots | 32 |
| Stack Length | 48.8mm | Number of rotor slots | 44 |
| Air gap length | 0.35mm | Number of poles | 4 |

varied from 2mm to 7mm in a step of 1mm, and the barrier positions from the rotor center were varied from 15mm to 30mm in a step of 5mm. However, the rib width of 0.5mm was maintained. Among 24 models, only 12 models can synchronize at full load, while the

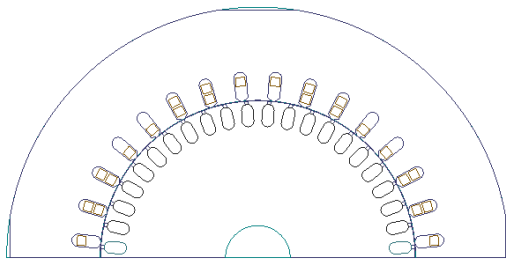


Figure 4. Single phase induction motor 2D geometry

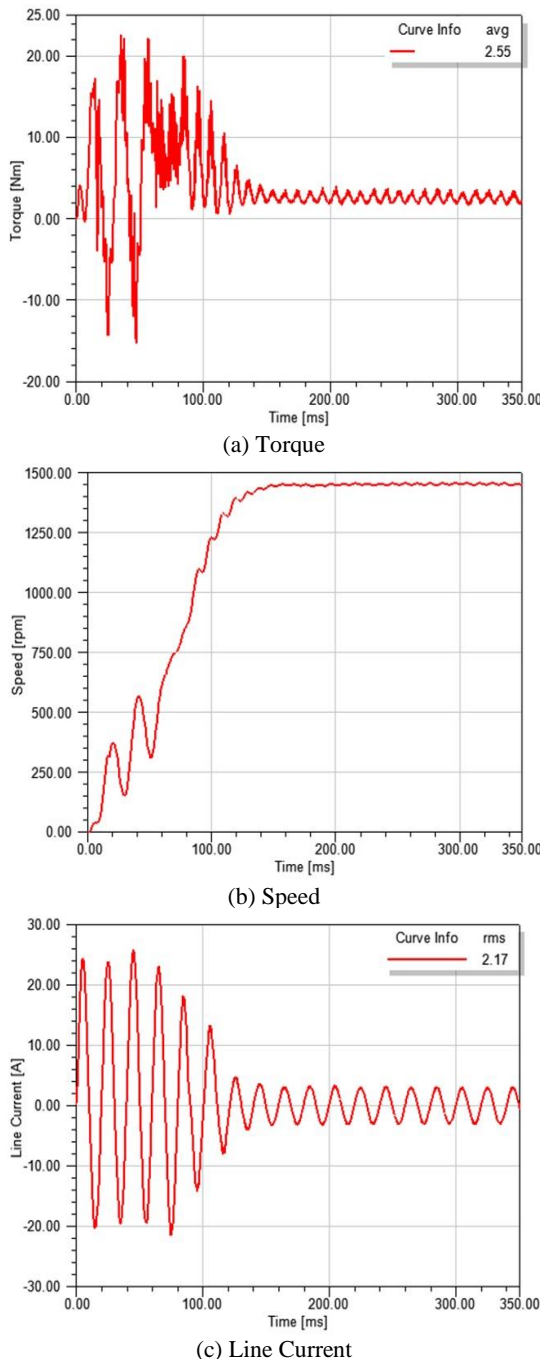


Figure 5. Performance results of single phase induction motor

other models are unable to develop required reluctance torque at full load. It is due to the fact that the synchronization capability depends on the developed reluctance torque.

It has been observed that the barrier width of 2mm leads to synchronization for each barrier position. Figure 6 describes the torque, efficiency, and total loss variations concerning the barrier positions.

Compared to the 25mm barrier position, the evaluated torque is highest at 15mm at a 3% decrease in efficiency. It is due to an increase of 16.96% in copper losses in the case of a 15 mm barrier position. The increase in the pulsating torque also leads to higher core losses. For the 25 mm barrier position, the highest efficiency of 82.04% with a mechanical power output of 393.67 W (higher than SPIM due to an increase in the speed of LS-SynRM) has been recorded.

Figure 7 shows the reluctance torque for barrier width 2mm and position of 25mm. The average torque was 2.5 Nm. The copper and core losses noted in this case were 42.42W and 35.5W, respectively. The better reluctance torque of 2.48Nm, as shown in Figure 7, has also been observed with the reduction in torque pulsation.

4. 2. 2. Performance without Rib

Considering the better performance at a barrier position of 25mm and width 2mm, the performance without a rib, as shown in Figure 8, has also been investigated. The significant reduction of 15% in torque ripples, as shown in Figure 9(a), has been recorded compared to a barrier with rib. However, the settling time, in this case, found increased, as shown in Figure 9(b). Also, a reduction of 2% in the total losses increases the efficiency by 0.4%. The average torque developed remains consistent in both cases with and without barrier rib.

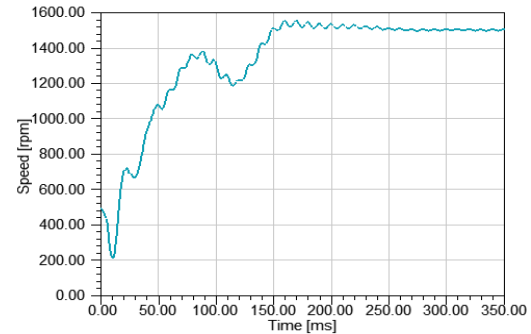
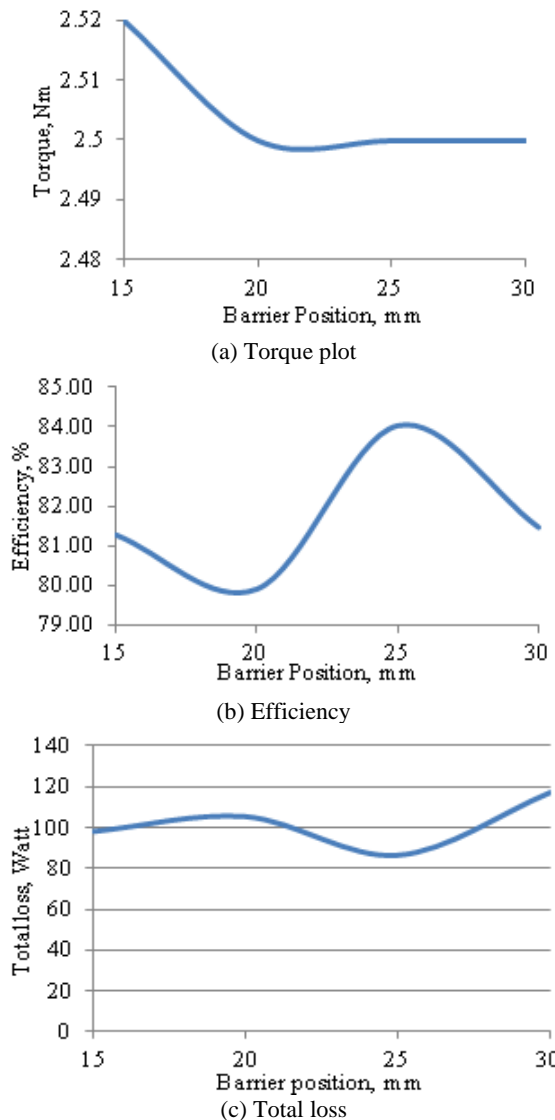


Figure 6. Performance plots with respect to barrier positions for 2mm width

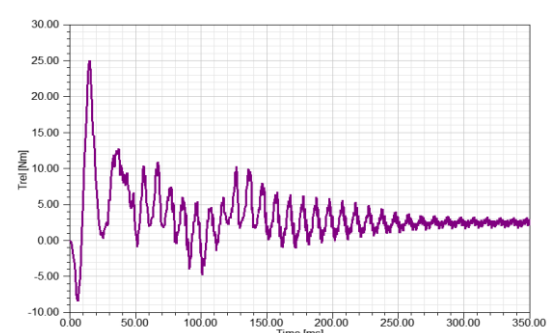


Figure 7. T_{rel} for barrier width 2mm and position of 25mm

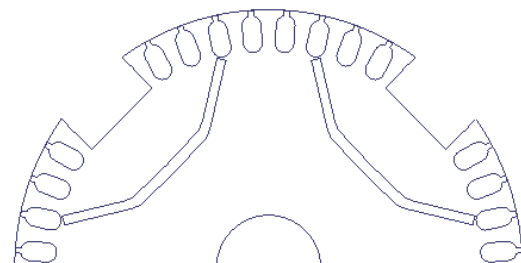


Figure 8. Barrier without rib

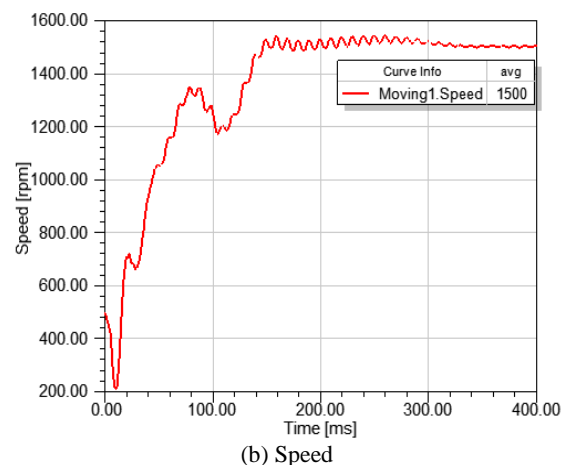
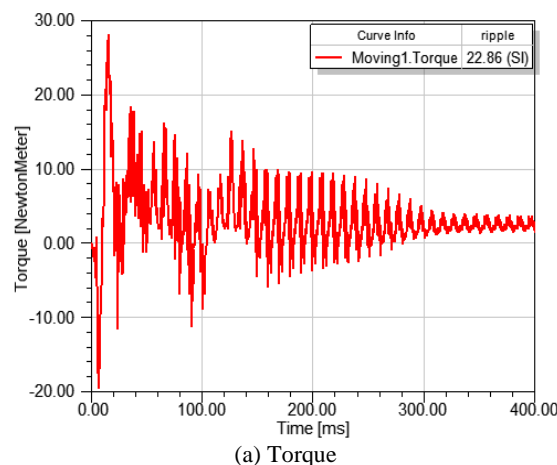


Figure 9. Plots of torque and speed for zero rib width

4. 2. 3. PM assisted LS-SynRM (PMaLS-SynRM)

Considering better performance with the introduction of permanent magnets (PM) [25], further investigations have been carried out with PMs in the rotor barrier. A NdFe30 PM type was used to analyze the same barrier position and width without rib, as shown in Figure 2(b). However, models with different sizes of PMs in the barrier analyzed for overall performance. Table 2 describes the results.

It has been observed that there is an increase in the efficiency with the length of PM. It was least for a length of 4mm and maximum for a length of 12mm. It is due to the reduction of the line current and the subsequent decrease in the copper losses. It has also been inferred from Figure 10, that the torque ripples increase with the length of the PM. However, the developed torque was consistent in all the designated cases for analysis.

Table 3 describes the analysis of stator and rotor core losses. The stator and rotor core losses decrease with the increase in PM length. However, the significant contributor to the core losses is the stator. These results are also consistent with the main and auxiliary winding current findings. The main winding current for the PM size of 12 mm is the lowest in all investigated cases.

Figure 11 demonstrates the torque and speed variation plots for PMaLS-SynRM. It is observed that the early synchronization(250ms) is achieved in the case of PMaLS-SynRM compared with LS-SynRM (325ms).

Figure 12 shows the speed plot under variable loading pattern for the best fit PMaLS-SynRM. At point 'a', the load torque is 1.8N-m (75% of rated load). However, it has increased to 2.4Nm (100% load, point 'b') at 400ms. The motor took 70ms to synchronize after the sudden dip (at point 'b').

TABLE 2. Performance of PMaLS-SynRM as function of size of PM

| Barrier Position (mm) | PM size (mm) | P _{mech} (W) | P _{elect} (W) | I _L (A) | P _{cu} (W) | P _{core} (W) | Other loss (W) | Total loss (W) | Efficiency (%) |
|-----------------------|--------------|-----------------------|------------------------|--------------------|---------------------|-----------------------|----------------|----------------|----------------|
| 15.00 | 4.00 | 396.31 | 485.15 | 2.21 | 43.67 | 36.45 | 8.72 | 88.84 | 81.69 |
| | 8.00 | 397.96 | 482.10 | 2.15 | 40.50 | 34.89 | 8.76 | 84.14 | 82.55 |
| | 12.00 | 396.52 | 477.72 | 2.11 | 38.12 | 34.36 | 8.72 | 81.20 | 83.00 |
| 20.00 | 4.00 | 394.93 | 482.24 | 2.18 | 43.67 | 34.95 | 8.69 | 87.31 | 81.90 |
| | 8.00 | 395.08 | 477.87 | 2.13 | 40.14 | 33.95 | 8.69 | 82.79 | 82.68 |
| | 12.00 | 398.86 | 479.86 | 2.13 | 38.61 | 33.61 | 8.77 | 81.00 | 83.12 |
| 25.00 | 4.00 | 400.32 | 479.48 | 2.12 | 37.48 | 32.87 | 8.81 | 79.16 | 83.49 |
| | 8.00 | 393.00 | 469.49 | 2.09 | 35.38 | 32.47 | 8.65 | 76.49 | 83.71 |
| | 12.00 | 401.12 | 477.51 | 2.14 | 34.96 | 32.61 | 8.82 | 76.39 | 84.00 |
| 30.00 | 4.00 | 393.62 | 483.70 | 2.19 | 44.86 | 36.56 | 8.66 | 90.08 | 81.38 |
| | 8.00 | 397.68 | 481.82 | 2.13 | 40.14 | 35.25 | 8.75 | 84.14 | 82.54 |
| | 12.00 | 396.15 | 476.36 | 2.09 | 37.32 | 34.17 | 8.72 | 80.21 | 83.16 |

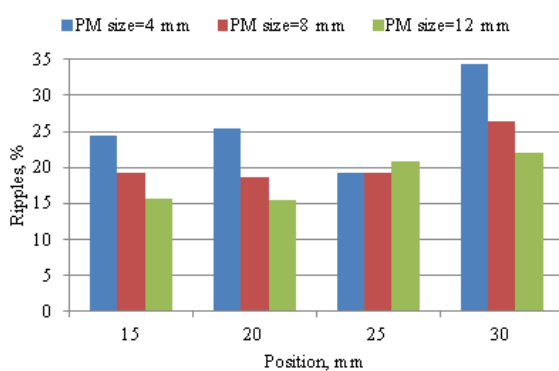


Figure 10. Torque ripple as a function of PM position and size

The comparative efficiency curves of LS-SynRM and PMaLS-SynRM at different loadings are shown in

TABLE 3. Losses in PMaLS-SynRM

| Barrier Position (mm) | PM length (mm) | I _m (A) | I _a (A) | P _{core-S} (W) | P _{core-R} (W) |
|-----------------------|----------------|--------------------|--------------------|-------------------------|-------------------------|
| 15.00 | 4.00 | 1.80 | 1.36 | 32.56 | 3.88 |
| | 8.00 | 1.63 | 1.36 | 31.25 | 3.64 |
| | 12.00 | 1.49 | 1.36 | 30.87 | 3.48 |
| 20.00 | 4.00 | 1.80 | 1.36 | 31.10 | 3.85 |
| | 8.00 | 1.61 | 1.36 | 30.38 | 3.57 |
| | 12.00 | 1.52 | 1.36 | 30.27 | 3.34 |
| 25.00 | 4.00 | 1.45 | 1.36 | 29.52 | 3.35 |
| | 8.00 | 1.31 | 1.36 | 29.29 | 3.18 |
| | 12.00 | 1.28 | 1.36 | 29.40 | 3.21 |
| 30.00 | 4.00 | 1.86 | 1.36 | 32.47 | 4.09 |
| | 8.00 | 1.61 | 1.36 | 31.66 | 3.59 |
| | 12.00 | 1.44 | 1.36 | 30.90 | 3.27 |

Figure 13. Both of these motors operate at the highest efficiency under full load. However, the efficiency of PMaLS-SynRM is 2% more than the LS-SynRM.

4.3. Comparative Analysis Table 4 presents the performance comparison of the three motors, viz. SPIM, LS-SynRM, PMaLS-SynRM. The PMaLS-SynRM has the highest efficiency of 84 %, which is 4% more than the base SPIM. The significant reduction(60% compared with base SPIM) in the copper loss in

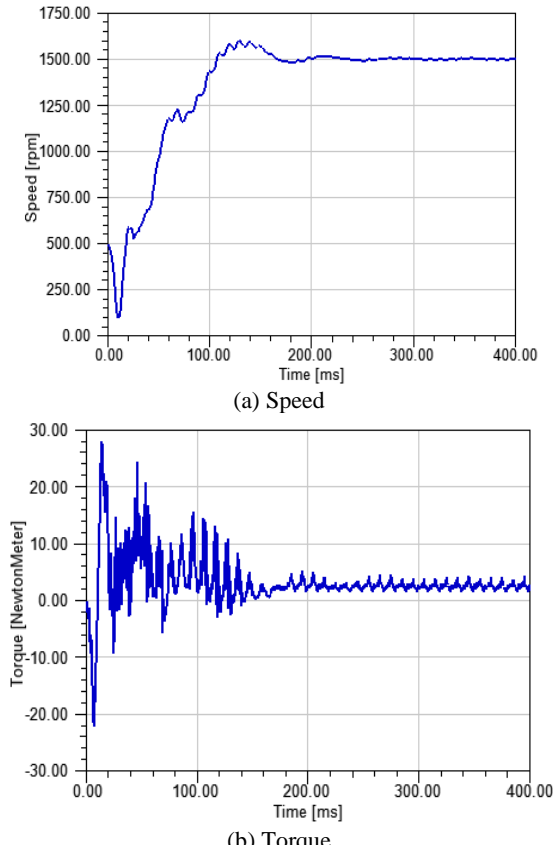


Figure 11. Speed and torque plot for best fit PM size

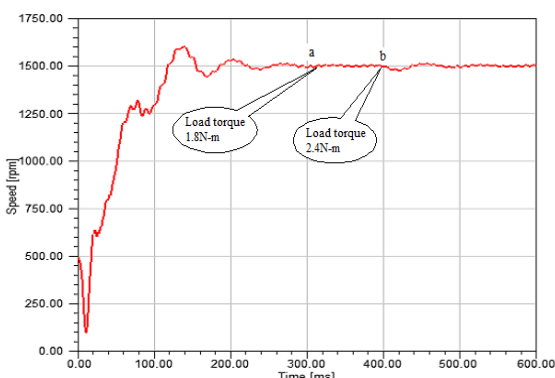


Figure 12. Speed transients at different load conditions

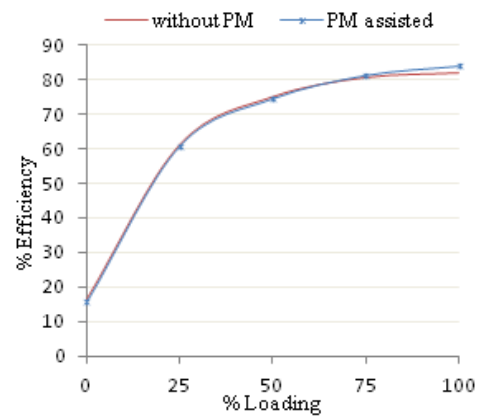


Figure 13. Efficiency plot

PMaLS-SynRM is also evident in this case. The core loss is also decreased in this case, although it is more compared with the base SPIM. However, the torque performance registered by all these three motors was the consistent and comparative analysis of the three motors is described in Table 4. It is observed that the torque developed by the three motors is nearly equal.

The analysis of the active material requirement in the motor reveals that PMaLS-SynRM requires 10% less material than the base SPIM.

The techno economic comparison also reveals the proposed conversion is still better option for efficiency improvement. Considering the current pricing, the average cost of 0.5hp SPIM is 74 USD, and the proposed conversion cost of the motor is 90 USD, including the cost of permanent magnets. Assuming flat 12 hours of daily motor operation and an energy rate of 0.106 USD per unit, the energy cost evaluated was 214.4 USD/Year and 204.5 USD/Year for SPIM and proposed PMaLS-SynRM. The proposed conversion will thus lead to energy saving of 10 USD/Year even for such a low power rated machine due to enhanced efficiency (4%). The significantly less payback time of 1.5 years thus leads to an attractive solution instead of replacing conventional SPIM with high-cost PMSM.

TABLE 4. Comparative results for three investigated motors

| Parameter | SPIM | Ls-SynRM | PmaLS-SynRM |
|------------------------|-------|----------|-------------|
| Torque (Nm) | 2.5 | 2.55 | 2.55 |
| Speed (rpm) | 1447 | 1500 | 1500 |
| Core loss (Watts) | 31.72 | 35.2 | 32.51 |
| Copper loss (Watts) | 56 | 42.32 | 34.96 |
| Efficiency (%) | 80.05 | 82.04 | 84 |
| Magnetic material(pu.) | 0.86 | 0.78 | 0.8 |
| Aluminum(pu.) | 0.13 | 0.1 | 0.1 |

5. CONCLUSION

The results of parametric design to convert the existing SPIM to LS-SynRM to enhance the overall performance have demonstrated that the barrier position and their width significantly affect the motor performance. The 25 mm barrier position and 2mm width have resulted in an efficiency of 82.04% for LS-SynRM, along with the reduction in torque pulsations. The best-fit barrier without a rib has further improved the performance in terms of efficiency and torque ripples. The rise of 0.4% efficiency has been recorded for the same motor.

However, the insertion of a permanent magnet in the barrier largely affected the overall motor performance. The efficiency noted, in this case, was maximum and is 84.04 % for the 12mm PM size. The significant rise of 4% in efficiency compared with the base motor has been evident in this case. It has also been observed that the efficiency increases significantly with the PM size at the cost of slightly inferior torque performance. It indicates the trade-off between the efficiency and ripples for selecting optimum PM dimensions.

The analysis through these extensive simulations has revealed that the conversion of existing SPIM is a better and more cost-effective option for performance improvement than the replacements. However, the PMaLS-SynRM is a suitable motor for constant speed applications.

6. REFERENCES

1. De Almeida, A.T., Ferreira, F.J. and Baoming, G., "Beyond induction motors—technology trends to move up efficiency", in 49th IEEE/IAS Industrial & Commercial Power Systems Technical Conference, IEEE., (2013), 1-13.
2. Yetgin, A.G. and Turan, M., "Efficiency optimization of slotted-core induction motor", *Journal of Electrical Engineering*, Vol. 65, No. 1, (2014), 60, doi: 10.2478/jee-2014-0009.
3. Verucchi, C., Ruschetti, C., Giraldo, E., Bossio, G. and Bossio, J., "Efficiency optimization in small induction motors using magnetic slot wedges", *Electric Power Systems Research*, Vol. 152, (2017), 1-8, doi: 10.1016/j.epsr.2017.06.012.
4. Ganesan, L.J., Jeyadevi, S. and Selvaraj, D.E., "Energy efficient single phase induction motor", (2013), doi: 10.1049/cp.2013.2222.
5. Ghosh, P.K., Sadhu, P.K., Basak, R. and Sanyal, A., "Energy efficient design of three phase induction motor by water cycle algorithm", *Ain Shams Engineering Journal*, Vol. 11, No. 4, (2020), 1139-1147, doi: 10.1016/j.asej.2020.01.017.
6. Alolah, A. and Badr, M., "Starting of three-phase reluctance motors connected to a single phase supply", *IEEE Transactions on Energy Conversion*, Vol. 7, No. 2, (1992), 295-301, doi: 10.1109/60.136224.
7. Badr, M. and Alolah, A., "Transient analysis of three phase reluctance motors fed from a single phase supply", *IEE Proceedings-Electric Power Applications*, Vol. 142, No. 2, (1995), 104-112, doi: 10.1049/ip-epa:19951702.
8. Chaudhari, B. and Fernandes, B., "Performance of line start permanent magnet synchronous motor with single-phase supply system", *IEE Proceedings-Electric Power Applications*, Vol. 151, No. 1, (2004), 83-90, doi: 10.1049/ip-epa:20030849.
9. Gwoździec, M. and Zawilak, J., "Single-phase line start permanent magnet synchronous motor with skewed stator", *Power Electronics and Drives*, Vol. 1, (2016), doi: 10.5277/PED160212.
10. Salehinai, S., Afjei, E., Hekmati, A. and Aghazadeh, H., "Design procedure of an outer rotor synchronous reluctance machine for scooter application", *International Journal of Engineering, Transactions C: Aspects* Vol. 34, No. 3, (2021), 656-666, doi: 10.5829/ije.2021.34.03c.10.
11. Siadatan, A., Rafiee, M. and Afjei, E., "Design, construction and comparison of a sensorless driver circuit for switched reluctance motor", *International Journal of Engineering, Transactions A: Basics* Vol. 27, No. 1, (2014), 143-156, doi: 10.5829/idosi.ije.2014.27.01a.17.
12. Stephenson, J. and Jenkinson, G., "Single-phase switched reluctance motor design", *IEE Proceedings-Electric Power Applications*, Vol. 147, No. 2, (2000), 131-139, doi: 10.1049/ip-epa: 20000176.
13. Higuchi, T., Fiedler, J.O. and De Doncker, R., "On the design of a single-phase switched reluctance motor", in IEEE International Electric Machines and Drives Conference, 2003. IEMDC'03., IEEE., (2003), 561-567.
14. Yoneoka, Y. and Akatsu, K., "An optimized design of high-efficiency switched reluctance motor with single-phase input operation", in 2011 International Conference on Electrical Machines and Systems, IEEE., (2011), 1-6.
15. Qi, F., Scharfenstein, D., Weiss, C., Müller, C. and Schwarzer, U., "Motor handbook".
16. Kostko, J., "Polyphase reaction synchronous motors", *Journal of the American Institute of Electrical Engineers*, Vol. 42, No. 11, (1923), 1162-1168, doi: 10.1109/JoAIEE.1923.6591529.
17. Finch, J. and Lawrenson, P., "Asynchronous performance of single-phase reluctance motors", in Proceedings of the Institution of Electrical Engineers, IET, Vol. 126, (1979), 1249-1254.
18. Chang, S., "An analysis or unexcited synchronous capacitor motors", *Transactions of the American Institute of Electrical Engineers*, Vol. 70, No. 2, (1951), 1978-1982, doi: 10.1109/EE.1952.6437948.
19. Gu, K. and Zhou, E., "Calculation and analysis for a new type of single-phase reluctance motor", *Electric Machines and Power Systems*, Vol. 15, No. 3, (1988), 163-176, doi: 10.1080/07313568808909329.
20. Obe, E. and Ojo, O., "Line-start performance of single-phase synchronous reluctance motor with controlled capacitor", *IEE Proceedings-Electric Power Applications*, Vol. 152, No. 4, (2005), 967-976, doi: 10.1049/ip-epa:20055208.
21. Ganesan, A.u. and Natesan Chokkalingam, L., "Single-phase direct-on-line synchronous motor for a specific application in comparison with an induction motor", *International Transactions on Electrical Energy Systems*, Vol. 29, No. 4, (2019), e2809, doi: 10.1002/etep.2809.
22. Finch, J. and Lawrenson, P., "Synchronous performance of single-phase reluctance motors", in Proceedings of the Institution of Electrical Engineers, IET, Vol. 125, (1978), 1350-1356.
23. Aghazadeh, H., Afjei, E. and Siadatan, A., "Comprehensive design procedure and manufacturing of permanent magnet assisted synchronous reluctance motor", *International Journal of Engineering, Transactions C: Aspects* Vol. 32, No. 9, (2019), 1299-1305, doi: 10.5829/ije.2019.32.09c.10.

24. Miller, T.J., "Single-phase permanent-magnet motor analysis", *IEEE Transactions on Industry Applications*, No. 3, (1985), 651-658, doi: 10.1109/TIA.1985.349722.
25. Parivar, H. and Darabi, A., "An improvement on slot configuration structure of a low-speed surface-mounted permanent magnet synchronous generator with a wound cable winding", *International Journal of Engineering, Transactions C: Aspects*, Vol. 34, No. 9, (2021), doi: 10.5829/ije.2021.34.09c.01.

Persian Abstract

چکیده

بهره وری انرژی یک جنبه ضروری از فن آوری های موتور است. جایگزینی موتور القایی تک فاز معمولی (SPIM) با موتور سنکرون مغناطیس دائم (PMSM)، موتور رلوکتانس سنکرون (SynRM) یا موتور رلوکتانس سوئیچ شده (SRM) برای عملکرد کارآمد انرژی منجر به هزینه های سرمایه ای بالایی می شود. این مقاله یک روش طراحی مقرون به صرفه برای بهبود کارایی SPIM موجود ارائه می کند. این ایده جدید را با تبدیل آن به موتور عدم تمایل همزمان شروع خط (LS-SynRM) پیاده سازی می کند. روتور ۰.۵ اسب بخار، SPIM با موفقیت با استفاده از تجزیه و تحلیل المان محدود (FEA) دوباره طراحی شد. تجزیه و تحلیل حساسیت پارامتریک جامع از نظر موقعیت مانع و عرض متمرکز بر کار. علاوه بر این، معرفی یک آهنربای دائمی در مانع روتور نیز مورد بررسی قرار گرفته است. تجزیه و تحلیل پارامتری اندازه بهینه آهنربای دائمی را تعیین می کند. با این حال، بهترین تناسب پارامترهای روتور قابل توجه تخمین زده شده است. نتایج بهبود قابل توجهی را در عملکرد LS-SynRM مشتق شده و SynRM با کمک مغناطیس دائمی نشان داد.
